Fermiology of Two-Dimensional Lateral Superlattices

C. Albrecht, J. H. Smet, D. Weiss,* and K. von Klitzing

Max-Planck-Institut für Festkörperforschung, D-70569 Stuttgart, Germany

R. Hennig, M. Langenbuch, M. Suhrke, and U. Rössler

Institut für Theoretische Physik, Universität Regensburg, D-93040 Regensburg, Germany

V. Umansky

Braun Center for Submicron Research, Weizmann Institute of Science, Rehovot 76100, Israel

H. Schweizer

IV Physikalisches Institut, Universität Stuttgart, D-70550 Stuttgart, Germany
(Received 11 February 1999)

We present magnetotransport experiments on high mobility two-dimensional electron systems subjected to a weak, short period superlattice potential. The imposed periodic potential modifies the contours of constant energy of the free electrons such that new closed k-space trajectories, involving magnetic breakdown, become possible. Their existence is heralded by a novel type of low-field quantum oscillations.

Tailoring the band gap along one spatial dimension by stacking a skillfully chosen sequence of semiconductors with different band gaps to produce new materials and devices with modified electronic and optical properties has reached a high degree of sophistication. Vertical superlattices are a well established example for altering the electronic properties and band structure. The dispersion in the vertical direction is determined by the artificial periodicity and the coupling between successive quantum wells rather than by the properties of the individual semiconductor layers [1]. Its generalization, that is, an artificial crystal with a tunable band structure in all spatial degrees of freedom, as the ultimate goal was envisaged in the 1970s. A two-dimensional electron system (2DES) on which a periodic square lattice potential is superimposed may be one possible route to achieve this target. The period of the lattice and the amplitude of the periodic modulation are adjustable parameters to engineer the width of the minibands and the minigaps [2]. Early attempts to realize and detect the electronic miniband structure on 2DES where the periodic potential was introduced by grid-shaped top gates displayed a modified conductance due to the superlattice, but it turned out to be difficult to nail down clear miniband effects [3]. In order to resolve the miniband structure it is necessary (i) to reduce the periods of the superlattice to length scales comparable to the Fermi wavelength of the electrons (~50 nm in GaAs heterojunctions), (ii) to have a 2DES close enough to the surface in order to impose a sufficiently strong potential modulation via patterned top gates, e.g., and (iii) to employ homogeneous, high mobility 2DES such that broadening due to impurities and inhomogeneities does not obscure the minibands. Here, we report clear evidence of the band structure induced by a 2D lateral superlattice. The periodic density modulation was introduced by means of patterned top gates. The miniband structure formation is manifested by modified Shubnikov–de Haas oscillations (SdH oscillations) of strikingly higher periodicity. While related modified SdH oscillations have been reported for transport experiments on vicinal surfaces with 1D periodicity [4,5], their observation has been illusive in 2D lateral superlattices so far.

The samples are prepared from a high-mobility GaAs-AlGaAs heterojunction, located 48 nm underneath the crystal surface. Prior to electron-beam lithography, the carrier density n_s and electron mobility μ are 3.0×10^{11} cm^{-2} and 2.1×10^6 cm^2/V s, corresponding to an elastic mean free path $l_F = 19$ μm. The samples are shaped into Hall bar geometries using standard photolithographic techniques. The 2D lateral modulation potential is implemented using a metallic top gate covering a grid-shaped electron-beam resist layer, containing holes with a diameter of approximately 50% of the lattice period a. This patterned resist layer, working as a template for the metallic gate, has a thickness of 180 nm. The lattice period is either 100 or 120 nm. The average areal density can be tuned by applying a bias voltage on the top gate. This bias voltage hardly affects the modulation strength, because a strong intrinsic modulation is present due to, e.g., mechanical stress originating from the different thermal expansion coefficients of the patterned gate and the semiconductor underneath [6]. Four-point magnetoresistance measurements were carried out in a dilution refrigerator using standard ac lock-in techniques with the external magnetic field applied perpendicular to the two-dimensional electron gas.

For a 120 nm lattice Fig. 1 depicts a typical measurement of the longitudinal resistance R_{xx} and Hall resistance R_{xy} at zero gate bias. The following magnetotransport
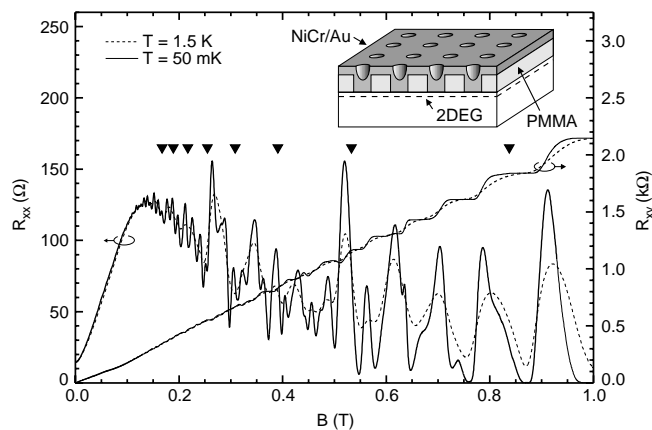
FIG. 1. Longitudinal resistance R_{xx} and Hall resistance R_{xy} for a 2D superlattice with period $a = 120$ nm for two temperatures [7]. The triangles indicate the flat band positions. The top inset shows a sketch of the lateral superlattice on top of the heterojunction [7].

phenomena can be observed in R_{xx}: a well developed positive magnetoresistance around zero magnetic field with a saturation field B_0 of 0.145 T and three types of $1/B$ periodic oscillations. The latter can be identified more clearly after replotting the data as a function of the inverse magnetic field, as shown in Fig. 2. At the higher fields, in region 1, the influence of the modulation potential is strongly suppressed and the usual SdH oscillations are observed. From their period $\Delta(1/B)_{\mathrm{SdH}} = 0.170$ T^{-1} we extract an areal density of 2.84×10^{11} cm^{-2}. In region 2, the SdH oscillations are superimposed on top of the well-known semiclassical commensurability oscillations [8–10]. These display minima for the flat band condition,

$$2R_{\mathrm{c}} = a(\lambda - 1/4), \qquad (1)$$

where λ is an integer and R_{c} is the cyclotron radius. Their period is $\Delta(1/B)_{\mathrm{FB}} = 0.682/$T. Finally, in region 3 unexpected oscillations show up with a distinct $1/B$ periodicity $\Delta(1/B)_{\mathrm{novel}} = 0.313/$T, which fits neither the periodicity of the SdH oscillations nor the periodicity of the commensurability oscillations for the given areal density. Their amplitude is modulated by the above mentioned semiclassical commensurability oscillations [11]. These novel oscillations, reported in preliminary form previously [12], are the subject of this Letter. It will be shown that the miniband structure induced by the electrostatic modulation needs to be invoked to account for these oscillations. Moreover, there exists an intimate connection with the mechanism of semiclassical magnetic breakdown [13,14].

The novel oscillations develop in the transition region between the positive magnetoresistance and the onset of the SdH oscillations. Two models have been put forward to describe the positive magnetoresistance and its saturation. Previous experiments were best explained within a classical model [15]. For magnetic fields where the electrical force due to the modulation potential is greater than the Lorentz force, electrons

may be trapped in the minima of the potential and runaway orbits in real space cause the positive magnetoresistance. It saturates when the magnetic force exceeds the electrical force. A second approach, relevant for the case at hand, is the semiclassical theory of magnetic breakdown [13]. Electrons suffer Bragg reflections at the boundaries of the Brillouin zone defined by the periodic potential. The free electron energy dispersion is perturbed and displays energy gaps at these boundaries. Under the influence of the magnetic field electrons move on constant energy contours in k space. In real space the corresponding path has the same shape, yet is rotated by $\pi/2$ and scaled by $\hbar/eB$. As a consequence of the Bragg reflections, the motion of electrons at the Fermi energy is modified and two classes of orbits coexist: closed orbits and undulating open runaway trajectories (Fig. 3b). As in the classical model, the latter enhance the magnetoresistance. Transitions between these different orbits would require the crossing of the energy gap at the Brillouin zone boundary. This tunneling is made possible by increasing the magnetic field [13]. The probability for tunneling becomes significant when the cyclotron energy $\hbar\omega_c$ reaches a value close to the relevant energy gap ΔE. If the tunneling rate is sufficiently large, the positive magnetoresistance saturates. Electrons now predominantly describe closed trajectories in k space—resembling the well-known cyclotron orbits for the case without modulation—by crossing the gaps instead of tracing the open orbits. This mechanism is called magnetic breakdown. It was introduced in the context of bulk metals [14].

With the reappearance of free cyclotronlike orbits the SdH oscillations develop. The Bohr-Sommerfeld quantization rule allows only closed orbits that enclose a quantized amount of magnetic flux. This restriction leads to the oscillatory behavior of quantities dependent on the density of states at the Fermi energy, such as the SdH oscillations in the longitudinal resistivity. Their period $\Delta(1/B)$ is inversely proportional to the area A_{F} in k space enclosed by
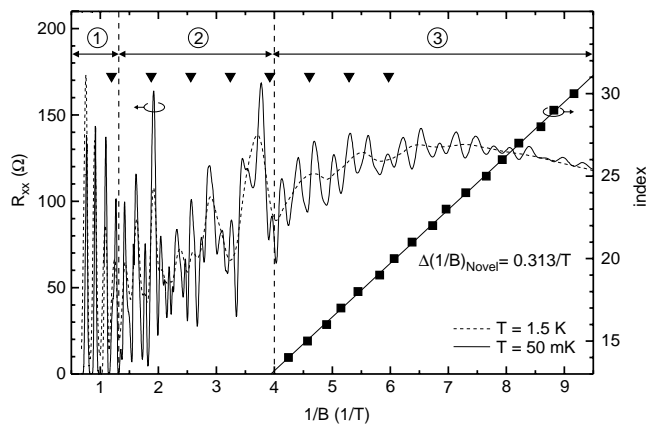
FIG. 2. Magnetoresistance as a function of the inverse magnetic field [7]. There are oscillations with three different $1/B$ periodicities. Triangles indicate flat band positions. The very regular oscillations in region 3 have a new fundamental period $\Delta(1/B)_{\mathrm{novel}}$.
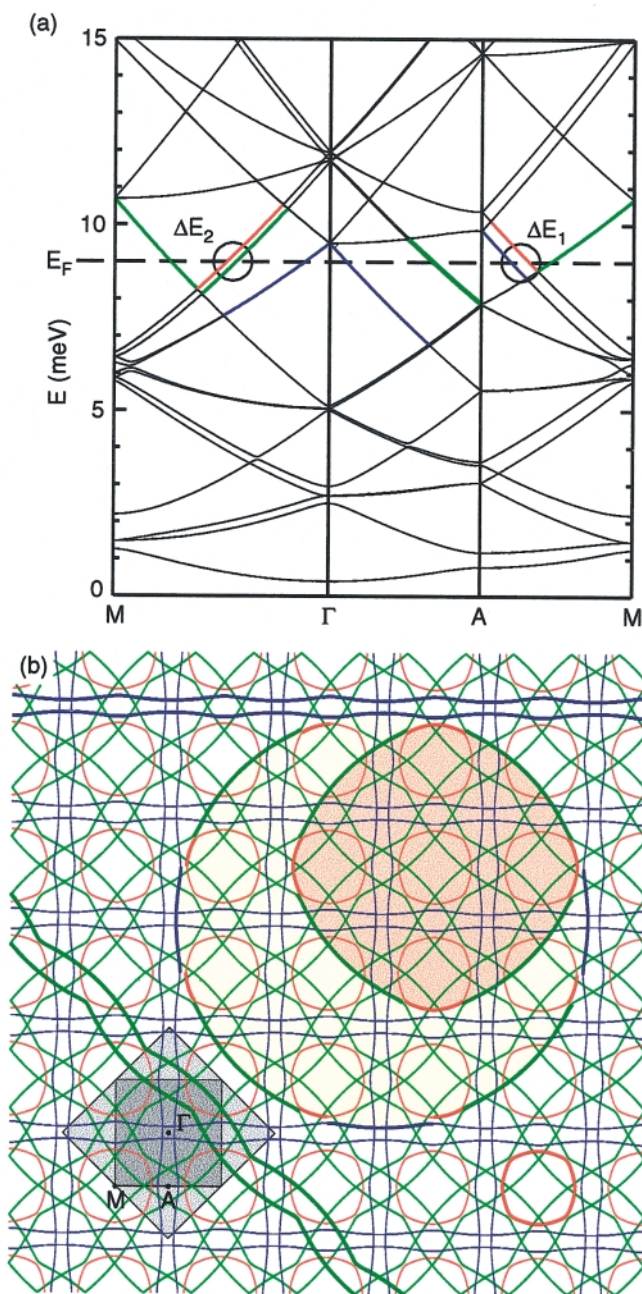
FIG. 3 (color). (a) Miniband structure of the weakly modulated 2DES with amplitude $V_0 = 2$ meV and period $a = 100$ nm of the modulation potential. The dashed line marks the energy position of the Fermi section in the lower plot. ΔE_1 and ΔE_2 are the main gaps at the Fermi energy due to the modulation potential. (b) Fermi section at $E_F = 9.0$ meV in the repeated zone scheme. The small red area and the large yellow shaded area determine the periodicity of the novel oscillations and the SdH oscillations, respectively. The dark and light shaded boxes in the lower left corner mark the first and second Brillouin zones.

the Fermi contour:

$$\Delta(1/B) = \frac{2\pi e}{\hbar} \frac{1}{A_F}. \qquad (2)$$

It will be shown that for the 2D lattice, prior to the appearance of the regular SdH oscillations, a different

closed orbit of constant energy E_F with a smaller area is more favorable and leads to the unexpected oscillations in region 3 with larger periodicity.

Theoretically we describe the modulated 2DES in the absence of a magnetic field within the effective mass approximation by the Hamiltonian

$$H = \frac{\mathbf{p}^2}{2m^*} + V_0 \left[\cos\left(\frac{\pi x}{a}\right) \cos\left(\frac{\pi y}{a}\right) \right]^2, \qquad (3)$$

with the effective mass m^* and a phenomenological potential of amplitude V_0 and lattice period a. To obtain the energy spectrum the Hamiltonian H is diagonalized using the basis of plane waves $e^{i(\mathbf{k}+\mathbf{G})\cdot\mathbf{r}}$, where $\mathbf{G}$ is a reciprocal lattice vector and $\mathbf{k}$ is a wave vector within the first Brillouin zone. Figure 3a shows an example of the miniband structure calculated for a lattice with period $a = 100$ nm and modulation amplitude $V_0 = 2.0$ meV. Two important energy gaps open up at the Brillouin zone boundaries: ΔE_1 and ΔE_2. In terms of the plane wave expansion of the electrostatic potential

$$V(\mathbf{r}) = \sum_{\mathbf{G}} \tilde{V}_{\mathbf{G}} e^{i\mathbf{G}\cdot\mathbf{r}}, \qquad (4)$$

the larger gap ΔE_1 is determined by the Fourier coefficients $\tilde{V}_{(\pm1,0)}$ and $\tilde{V}_{(0,\pm1)}$, whereas the smaller gap ΔE_2 is related to $\tilde{V}_{(\pm1,\pm1)}$. For the assumed amplitude $V_0 = 2.0$ meV and the Fermi energy $E_F = 9$ meV, they take on the values 0.5 meV and 0.25 meV, respectively.

The constant energy contours at the Fermi energy are depicted in Fig. 3b using the repeated zone scheme. Because of the appearance of energy gap ΔE_1 along the boundary of the first and energy gap ΔE_2 at the boundary of the second Brillouin zone, the Fermi surface is broken up into three important sets of disconnected contours: closed orbits (red colored) and two sets of undulating open contours that run along either the M-A (blue) or Γ-M (green) and their equivalent directions. In the limit of very weak magnetic fields, the motion of electrons at the Fermi energy proceeds exclusively along these continuous constant energy contours and the observed positive magnetoresistance around zero magnetic field arises from electrons moving along the open trajectories. With increasing field, this condition is relaxed and the finite probability for tunneling across the energy gaps allows transitions between the different contours. It modifies significantly the topology of the electron trajectories. Electrons can first overcome the smaller energy gap ΔE_2, which originally prevented transitions between the red and green contours. Thereby a closed path is formed. It is the above proposed orbit bringing about the oscillations with larger periodicity $\Delta(1/B)_{\text{novel}}$ in region 3 and encloses approximately half of the area in k space (red shaded area in Fig. 3b) in comparison with the cyclotron orbit for the case without 2D modulation. The larger yellow shaded area indicates the size of this cyclotron orbit in the unmodulated system. An orbit resembling this one is also possible in the modulated system; however, it is composed of segments of all three sets of contours. Therefore, its execution would require, besides tunneling across
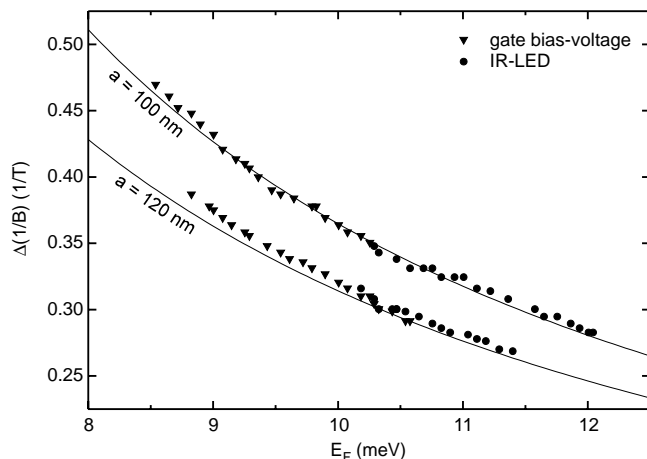
FIG. 4. $1/B$ periodicity of the novel oscillations as a function of the Fermi energy E_F for two lattice periods a. Experimental data are compared with the corresponding values from the calculated areas enclosed by the smaller orbit in k space.

ΔE_2, transitions between the red and blue contours separated by the larger energy gap ΔE_1. Thus, there is a range of magnetic fields where the trajectories encircling the smaller area A_{small} rule the transport properties and it is this area that determines the $1/B$ periodic oscillations here. The experimentally observed periodicity agrees well with the theoretical value obtained from the enclosed area in k space in Fig. 3b. Beyond a certain critical magnetic field the larger cyclotron orbits are restored and the regular SdH oscillations show up.

To further support our interpretation the periodicity was investigated as a function of carrier density n_s by either applying a bias voltage on the top gate or successive illumination of the sample with an infrared light-emitting diode. The results for two different lattice periods a are depicted in Fig. 4. Our calculations show that the precise amplitude of the modulation potential [16] does not alter significantly the predicted value of $\Delta(1/B)_{\mathrm{novel}}$ as well as its dependence on the carrier density, since the effect merely lives from the existence of energy gaps. The modulation amplitude sets only the size of the energy gaps and thereby the magnetic field range where the oscillations occur. In the limit of vanishing modulation amplitude the area A_{small} is given by

$$A_{\mathrm{small}}(k_F, a) = \pi k_F^2 + 4\left(\frac{\pi}{a}\right)^2 - 4\frac{\pi}{a}\sqrt{k_F^2 - \left(\frac{\pi}{a}\right)^2}$$
$$- 4k_F^2 \arcsin\frac{\pi}{ak_F}. \qquad (5)$$

The resulting theoretical values (solid curves in Fig. 4) for $\Delta(1/B)_{\mathrm{novel}}$ depend only on the lattice period a and the carrier density n_s via $k_F = \sqrt{2\pi n_s}$. The agreement is striking and makes a strong case for the theoretical explanation, which does not require any fitting parameters.

In summary, we have studied the fermiology of 2D superlattices and found unequivocal evidence for modifications to the contours of constant energy. Hitherto unobserved magnetoquantum oscillations mediated by magnetic breakdown ensue. Our experiment opens the way to study the quantum transport in bands defined by externally tunable paramaters like the geometry and modulation amplitude of the lateral superlattice.

---

*Present address: Institut für Experimentalphysik, Universität Regensburg, D-93040 Regensburg, Germany.
 [1] J.-K. Maan, Adv. Solid State Phys. **27**, 137 (1987), and references therein; T. Duffield *et al.,* Phys. Rev. Lett. **56**, 2724 (1986).
 [2] H. Sakaki *et al.,* Thin Solid Films **36**, 497 (1976); R. T. Bate, Bull. Am. Phys. Soc. **22**, 407 (1977); H. Sakaki, Jpn. J. Appl. Phys. **28**, L314 (1989).
 [3] G. Bernstein and D. K. Ferry, J. Vac. Sci. Technol. B **5**, 964 (1987); K. Ismail *et al.,* Appl. Phys. Lett. **54**, 460 (1989); for a review, see C. W. J. Beenakker and H. van Houten, Solid State Phys. **44**, 1 (1991).
 [4] T. Cole, A. A. Lakhani, and P. J. Stiles, Phys. Rev. Lett. **38**, 722 (1977); L. J. Sham *et al.,* Phys. Rev. Lett. **40**, 472 (1978); for a review, see T. Ando, A. B. Fowler, and F. Stern, Rev. Mod. Phys. **54**, 437 (1982).
 [5] For recent work on epitaxially overgrown vicinal surfaces, see H. Sakaki *et al.,* Physica (Amsterdam) **4E**, 56 (1999), and references therein.
 [6] J. H. Davies and I. A. Larkin, Phys. Rev. B **49**, 4800 (1994); I. A. Larkin *et al.,* Phys. Rev. B **56**, 15 242 (1997).
 [7] Reprinted from Physica (Amsterdam) **249B–251B**, C. Albrecht *et al.,* 914–917 (1998), with permission from Elsevier Science.
 [8] D. Weiss *et al.,* Europhys. Lett. **8**, 179 (1989); R. R. Gerhardts, D. Weiss, and K. von Klitzing, Phys. Rev. Lett. **62**, 1173 (1989).
 [9] R. W. Winkler, J. P. Kotthaus, and K. Ploog, Phys. Rev. Lett. **62**, 1177 (1989).
[10] E. S. Alves *et al.,* J. Phys. Condens. Matter **1**, 8257 (1989).
[11] In Fig. 2 at the higher temperature of 1.5 K only these commensurability features survive.
[12] C. Albrecht *et al.,* Physica (Amsterdam) **249B–251B**, 914 (1998).
[13] P. Streda and A. H. MacDonald, Phys. Rev. B **41**, 11 892 (1990).
[14] M. H. Cohen and L. M. Falicov, Phys. Rev. Lett. **7**, 231 (1961); R. W. Stark and L. M. Falicov, Prog. Low Temp. Phys. **5**, 235 (1967).
[15] P. H. Beton *et al.,* Phys. Rev. B **43**, 9980 (1991).
[16] For the case of a 2D modulation it is particularly difficult to extract an accurate value of the modulation amplitude from the experimental data. The saturation field B_0 of the positive magnetoresistance yields a rough estimate of about $0.5-1$ meV. For the sake of clarifying our theoretical picture, we have chosen a value of 2 meV, since otherwise the gaps between the different trajectories in Fig. 3b would hardly be visible on this scale.